Analysis of Spectrum-Imaging Datasets in Atomic-Resolution Electron Microscopy

Masashi Watanabe,[1] Eiji Okunishi [2] and Kazuo Ishizuka [3] 1. Department of Materials Science and Engineering, Lehigh University, Bethlehem, PA, USA. 2. JEOL, Tokyo, Japan. 3. HREM Research Inc., Saitama, Japan.

BIOGRAPHY

Masashi Watanabe has a BSc from Kyushu University and a PhD in metallurgy from Kyushu University. He is now an associate professor in the Department of Materials Science and Engineering at Lehigh University, Bethlehem, Pennsylvania. His research interest is the characterization of materials using various electron microscopy techniques including XEDS and EELS analysis in AEM and HAADF imaging in STEM.

ABSTRACT

Recently, a multivariate statistical analysis (MSA) package has been developed. In this article, the basic concept of principal component analysis (PCA), which is one of the most common MSA approaches, is described. An application of the package to an STEM atomic-column electron energy-loss spectrum-imaging dataset of Si_3N_4 is demonstrated. The PCA approach is very useful to identify statistically significant features that might be hidden under heavy random noise and to reduce efficiently random noise components. In addition, other useful auxiliary utilities available in the MSA package are briefly described.

KEYWORDS

transmission electron microscopy, scanning transmission electron microscopy, electron energy-loss spectroscopy, principal component analysis, atomic-column EELS, Si_3N_4, noise reduction, Wiener filter

ACKNOWLEDGEMENTS

The authors thank Prof. David Williams (currently at the Univ. of Alabama, Huntsville) for his thoughtful supervision during the development of the MSA plug-ins, and Kenta Yoshimura (HREM Research Inc.) for his support in the development of the MSA plug-ins. MW acknowledges the support of the National Science Foundation (grant DMR-0804528) and Bechtel Bettis, Inc.

AUTHOR DETAILS

Professor Masashi Watanabe, Dept. of Materials Science and Engineering, Lehigh University, 5 East Packer Ave, Bethlehem, PA18015, USA
Email: masashi.watanabe@lehigh.edu
Web: www.lehigh.edu/~maw3/index.html

Microscopy and Analysis 23(7):5-7 (AM), 2009

INTRODUCTION

Various properties of materials can frequently be controlled by fine compositional fluctuations on the nanoscale, such as the nano-precipitation or nucleation of secondary phases and segregation of impurities at boundaries and interfaces. Elemental and/or compositional mapping in scanning/transmission electron microscopy (S/TEM) is an essential approach to this problem because 2D elemental fluctuations in composition around such nanoscale features, which may be easily missed by conventional point or line-scan analysis, can be revealed as images, corresponding to local microstructures. Such elemental maps can be acquired by a static electron beam with energy-filtering TEM (EFTEM) or by a scanning electron beam in the STEM in conjunction with energy dispersive X-ray spectroscopy (EDS) and/or electron energy-loss spectroscopy (EELS). With the latest aberration-corrected S/TEM instruments, the spatial resolution of elemental mapping approaches the atomic scale [e.g. 1, 2].

The elemental mapping approach can be further expanded by spectrum imaging (SI), which stores a full spectrum at each pixel instead of choosing several energy windows prior to mapping [3,4]. Because a full spectrum is continuously recorded along the energy-channel (spectral) dimension, information regarding elements contained in the SI dataset may not be missed without prior knowledge. Now the SI method is available not only for STEM-based EELS and EDS, but also for EFTEM. Furthermore, the SI method offers post-acquisition treatment of elemental maps including regular spectral-processing techniques such as background subtraction and signal deconvolution. Therefore, it is now possible to map out unexpected minor elements that were not even considered beforehand for mapping if signals from such minor elements are successfully identified. However, in characterizing elemental fluctuations around nanoscale features, elemental mapping including SI in the S/TEM suffers from weak signals due to the smaller volume of material and the relatively shorter acquisition time for each pixel or for each energy channel.

Weak signals in elemental mapping can be enhanced by advanced statistical techniques such as multivariate statistical analysis (MSA), which has been successfully applied to SI datasets [5]. By applying MSA to SI datasets, statistically significant features that are dominant information in the datasets can be automatically extracted without prior knowledge, and noise-reduced datasets can be reconstructed by subtracting random noise components. The data reconstruction without random noise components results in the enhancement of weak signals in SI datasets. The MSA approach is an essential tool to handle large SI datasets efficiently. Recently, we developed the MSA software package as a series of plug-ins for a popular digital electron micrograph analysis software (Gatan DigitalMicrograph Suite, DMS), which is widely used to acquire and analyze EELS and EFTEM SI datasets. It should be noted that EDS SI datasets can also be acquired in DMS using other EDS systems.

In this article, the basic concept of principal component analysis (PCA) – one of the MSA processes and available in the MSA plug-ins – is first briefly described, and then a fundamental SI data analysis with PCA is demonstrated for the analysis of atomic-column EELS data. In addition to the MSA plug-in, this series of plug-ins consists of several useful utilities, which will also be briefly described.

METHODS

Applications of PCA to an SI dataset

MSA is a useful family of statistic-based techniques to analyze large datasets. PCA is one of the most popular MSA approaches and is also widely performed as a first step to other more advanced MSA approaches. The general concept of PCA is to reduce the dimensionality of an original large dataset by finding a minimum number of variables that describe the original dataset without losing any significant information [e.g. 6, 7].

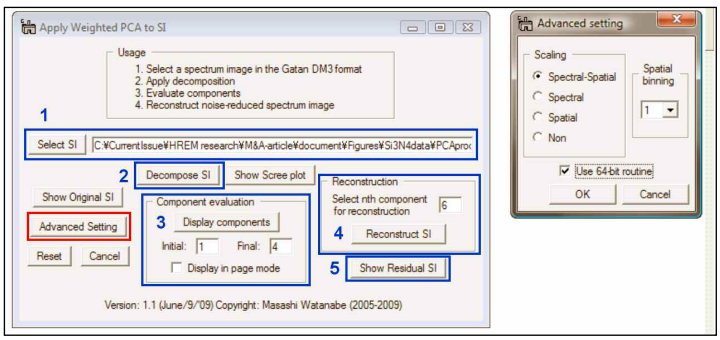

Figure 1: The main (left) and advanced setting (right) dialogs of the PCA plug-in in the MSA plug-ins package.

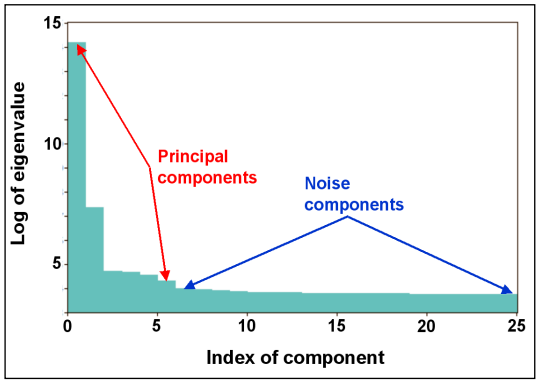

Figure 2 (left): An example of the scree plot generated after the PCA decomposition in the PCA plug-in.

Figure 3 (right): Pairs of loading spectra and score images of components #1 and #2 of the atomic resolution STEM-EELS SI dataset from Si_3N_4. of loading spectra and score images of components #1 and #2 of the atomic resolution STEM-EELS SI dataset from Si_3N_4.

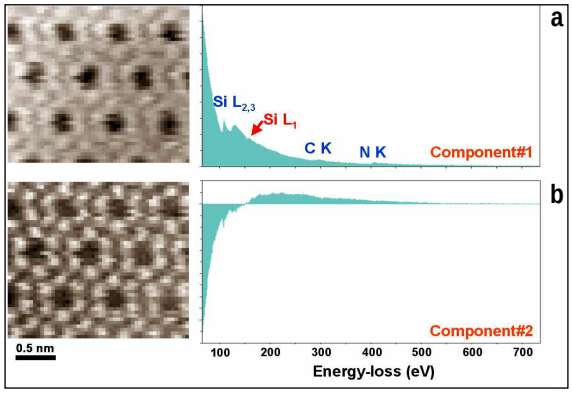

An SI dataset acquired as a 3D data cube with the spatial dimensions (x, y) and the spectral (energy channel) dimension E can be converted into a 2D data matrix $\mathbf{D}_{((x,y),E)}$. By applying PCA, this matrix can be decomposed as:

$$\mathbf{D}_{((x,y),E)} = \mathbf{S}_{((x,y),n)} \times \mathbf{L}^{T}_{(E,n)} \quad (1)$$

where $\mathbf{L}_{(E,n)}$ and $\mathbf{S}_{((x,y),n)}$ are called loading and score matrices, respectively. After the decomposition, each row of $\mathbf{L}$ contains a spectral feature uncorrelated to other row information, and each row of $\mathbf{S}$ represents the spatial amplitude of the corresponding loading spectrum. The superscript T of $\mathbf{L}$ indicates a matrix transpose. In practice, the above matrix decomposition can be performed by eigenanalysis or singular value decomposition to the data matrix $\mathbf{D}$ and provides not only decomposed matrices $\mathbf{L}$ and $\mathbf{S}$, but also eigenvalues of the data matrix. The individual product of each row of the loading and score matrices is called a component, and the number of the components n is mathematically equivalent to the rank of the data matrix $\mathbf{D}$, which is equal to or less than the smaller number of $(x \times y)$ or E.

This matrix decomposition is carried out by clicking the '*Decomposition*' button (designated as 2) in the weighted PCA dialog (Figure 1a) after the original SI data in the DMS dm3 format is assigned through the '*Select SI*' button (denoted as 1). Once the decomposition is completed, a scree plot that is a log of the eigenvalues plotted against the index of components is displayed (Figure 2). Note that all matrix treatments in the PCA plug-in are performed through Intel Math Kernel Libraries, which are optimized for most commercialized CPUs in both 32- and 64-bit modes. Although the current version of DMS is a 32-bit application, the PCA plug-in can run in the 64-bit mode under 64-bit Windows. The 64-bit-mode PCA program can handle larger SI datasets more efficiently since over 2 GB of memory space can be allocated as a single stack if such high memory space is freely available. The 64-bit mode can be activated in the advanced setting dialog as shown in Figure 1b. It is also noteworthy that appropriate pre-processing to SI datasets is essential prior to the matrix decomposition. As already discussed in the literature [8, 9], spatial- and spectral-scalings based on Poisson counting-statistics as preprocesses are essential for the MSA treatment on SI datasets. In the PCA plug-in, this scaling preprocess can be selected (both spatial- and spectral-scalings are default) in the advanced setting dialog (Figure 1b).

Principal Components of the SI Dataset

After the decomposition, dominant features of the data are stored in the loading and score matrices. These dominant features are called principal components (PCs), and typically a number of the PCs is far less than the rank of the data matrix n. The number of PCs can be determined by evaluating the magnitude of eigenvalues. One of the most common approaches is to use the scree plot as shown in Figure 2. The scree plot is a log of the eigenvalues of corresponding components plotted against the index of the components. The magnitude of each eigenvalue indicates an amount of variance that the corresponding component contributes to the dataset; i.e., the scree plot can be considered as a histogram representing the frequency (the number of times the individual features are repeated in the data matrix). Therefore, if the eigenvalue is high, the corresponding component should be statistically significant. Conversely, lower eigenvalues indicate that the corresponding components are not repeated in the data; i.e. random noise. Usually such random noise components appear as a plateau in the scree plot.

Unfortunately, it may be not very straightforward to judge the number of PCs from only the scree plot, especially when the difference in eigenvalues between the feature and noise components is sometimes very small. Therefore, near the plateau region in the scree plot, it is essential to evaluate each component in terms of a pair of a loading spectrum (spectral feature) and a score image (spatial amplitude) to distinguish the principal components from noise more accurately. In the PCA plug-in, the individual components with the desired range of component indices can be viewed by clicking the '*Display Components*' button (designated as 3 in Figure 1a).

RESULTS

Application to an Atomic-Resolution STEM-EELS SI Dataset from Si_3N_4

The PCA plug-in was applied to analyze a STEM-EELS SI dataset taken from Si_3N_4 in an aberration-corrected JEM-2100F instrument operated at 200 kV. The SI dataset was recorded with 50×45 pixels and 670 energy-channels (with 2×binning) using a Gatan Enfina spectrometer for a dwell time of 20 ms in atomic-resolution conditions along the [001] projection. The selected components obtained after the PCA decomposition are shown as pairs of the loading spectrum and the corresponding score image in Figure 3. The most significant component in the dataset is always the average (i.e. the average information is repeated at every pixel), and hence the loading spectrum of component #1 (Figure 3a) represents the average spectrum of the SI dataset. Characteristic edges of Si L, N K and C K can be seen in this SI dataset. Note that the C K edge signals came from contamination build-up during acquisition.

Any component higher than #1 indicates the difference from the average in the PCA process. Therefore, loading spectra after the component #1 contain positive and negative regions, which are not physically meaningful but interpretable expressions. The result of component #2 in this particular dataset seems very interesting, as shown in Figure 3b. The brighter regions in the score image of component #2 correspond to the Si atom positions. Surprisingly, this enhancement at Si atom positions occurs not at the Si $L_{2,3}$ edge, but after the Si L_1 edge as shown in the loading spectrum of component #2. The Si L_1 edge represents the *s* state of the electron configuration in a Si atom. In this particular case, therefore, the energy-loss process (i.e. inelastic scattering) is more localized around the *s* electron state rather than other electron states. Recently, Kimoto et al. [10] reported similar results: the Si L edge maps from Si_3N_4 show better spatial resolution at the higher energy-loss region than the map immediately after the ionization energy (i.e. Si $L_{2,3}$ map). This resolution difference in a different energy-loss region can be due to the delocalization-effect dependence on the offset energy from the ionization edge.

Obviously, more detailed discussions with theoretical assessments are required to interpret this L_1 edge enhancement at the Si atomic column. Such unique correlations of spectral features with specific spatial locations might not be identified accurately unless these correlations are well known prior to data acquisi-

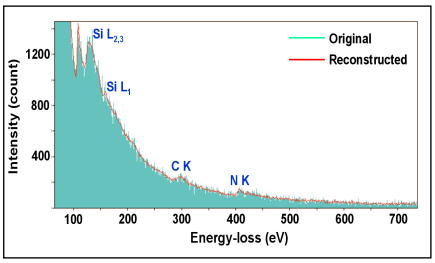

Figure 4: Comparison of EELS spectra at a single pixel extracted from the original and PCA-reconstructed SI datasets.

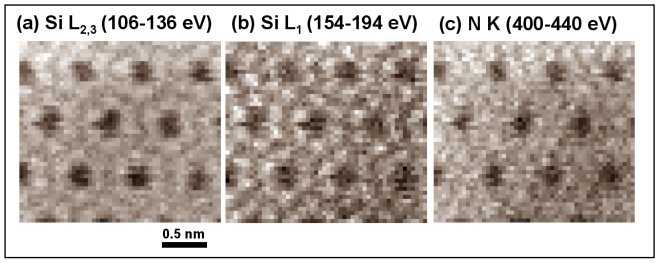

Figure 5:
Characteristic signal maps of the Si $L_{2,3}$ (a), Si L_1 (b) and N K edges (c) obtained from the PCA-reconstructed SI dataset with background subtraction.

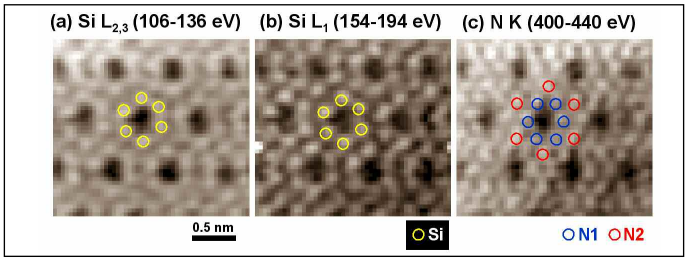

Figure 6: Characteristic signal maps of the Si $L_{2,3}$ (a), Si L_1 (b) and N K edges (c) modified from the maps in Figure 5 by applying the Wiener filter, which is available in the HREM-Filters Pro plug-ins. The Si positions and two types of N positions (denoted as N1 and N2) are overlaid in either the Si maps or the N map, respectively.

tion/analysis (this is why SI data are taken!). However, by applying PCA, these unexpected features can be automatically revealed.

Noise reduction of the SI dataset through PCA

After the PCs are distinguished from noise parts, the original SI dataset can be described with a limited number of the PCs, α, instead of the total rank of data matrix n:

$$\tilde{\mathbf{D}}_{((x,y),E)} = \mathbf{S}_{((x,y),\alpha)} \times \mathbf{L}^{T}_{(E,\alpha)} \qquad (2)$$

where $\tilde{\mathbf{D}}$ is the reconstructed data matrix with only the PCs up to the number of $\alpha(<< n)$. As a result of the data reconstruction, the random-noise parts can be efficiently removed from the original SI without degrading the spatial or energy resolution. The data reconstruction can be carried out by clicking the '*Reconstruct SI*' button (denoted as 4 in Figure 1a) with a selection of α. The data reconstruction can also be confirmed by evaluating the residual matrix calculated from the difference between the original and reconstructed data matrix denoted as 5 in Figure 1a.

In the atomic-resolution SI dataset from Si_3N_4, components up to the 6th can be distinguished as PCs from the scree plot shown in Figure 2. Thus, the data matrix can be expressed by the first 6 components instead of the rank of the matrix, 670. In Figure 4, a spectrum at a single pixel extracted from the reconstructed SI data (red line) is compared with the original spectrum at the same pixel position. This comparison of spectra from the original and reconstructed SI datasets clearly demonstrates the efficient removal of the noise. Conversely, the same intensity level is maintained at each energy-channel after the noise reduction.

Figure 5 shows three maps extracted from the reconstructed SI dataset with proper background subtraction: (a) the Si $L_{2,3}$ edge from the energy range of 106-136 eV; (b) the Si L_1 edge from 154-194 eV; and (c) the N K edge from 400-440 eV. The map of Si $L_{2,3}$ edge shows the intensity distribution of a six-fold ring, which corresponds to the Si atom arrangement along the [001] direction. This six-fold atom arrangement becomes much clearer in the Si L_1 map, and the individual Si atomic columns are clearly distinguished, as expected from component #2 shown in Figure 3b.

The N K map shows nearly homogeneous distribution except for the inside regions of the Si six-fold ring, where no atoms exist. However, the N atom positions both in the six-fold ring and between the rings might be seen especially at the top part of the map. The N K map was degraded by the carbon K edge signals caused by contamination build-up during data acquisition. N atom distributions would appear to be more evident without the contamination build-up.

The characteristic edge maps contain information of atomic positions: some positions are very clear while others are unclear as shown in Figure 5. To enhance the atomic-position information, the Wiener filter available in the HREM-Filter Pro plug-ins was applied to the edge maps, and the filtered maps are shown in Figure 6. After the Wiener filter is applied, the Si atom positions can be clearly identified, even in the Si $L_{2,3}$ edge map. The Si atom positions are superimposed on the nominal positions schematically overlaid in the Si $L_{2,3}$ and L_1 maps. In the [001] projected Si_3N_4, there are two types of N atom positions: one is on the six-fold ring and other is between the six-fold rings denoted as N1 and N2, respectively.

In the unfiltered N map (Figure 5c), the N atomic position is barely visible. Conversely, after applying the Wiener filter, both types of the N positions are visible (not superimposed on the Si positions). It should be noted that the N signals in the six-fold rings (N1) are not as clear as the signals between the rings (N2), which is caused by the difference in probe propagation at two different N columns as theoretically estimated by Kimoto et al. [10]. In the N1 atom position with neighbor Si atoms, electrons are more localized in the Si atom sites rather than in the N1 site. However, since the N2 site is relatively far from the heavier Si atoms, electrons tend to be localized in the N2 column.

Auxiliary Utilities in the MSA Plug-ins

In addition to the PCA plug-in mainly featured in this article, several auxiliary utilities are available in MSA plug-ins to handle SI datasets more efficiently.

SI datasets can also be acquired through other software packages instead of DMS. Most XEDS manufacturers now offer the SI acquisition function in the systems, or at least a series of XEDS spectra as a line profile can be acquired in any EDS system available. Three data import functions are currently available in the MSA plug-ins: (1) EMSA spectrum series import; (2) ED-SI data import;p and (3) EFTEM image series import. The first function imports a series of EMSA ([Electron]Microscopy Society of America)-formatted spectra into DMS as a 2D SI dataset (i.e. a line profile). The second function imports a SI dataset in a raw binary format, which could be saved in several EDS systems. The last function converts a series of individual EFTEM images acquired by the '*Acquire Filtered Series*' function in DMS to a SI dataset.

Furthermore, several functions to manipulate SI datasets are also available in the MSA plug-ins, e.g. pixel/channel binning (which are available in newer versions of DMS as well) and spatial/spectral data extraction. The data extraction functions of '*Spatial Sub SI*' and '*Spectral Sub SI*' are very useful to extract a new SI dataset from a selected spatial region or a selected energy-channel region of the existing SI dataset.

CONCLUSIONS

In this article, the basic concept of the PCA approach is described using the MSA plug-ins for Gatan DMS, and an application to an atomic-column STEM-EELS SI dataset from Si_3N_4 was demonstrated. As shown in the example, the PCA process may reveal unexpected information hidden in a SI dataset. Furthermore, random noise in the datasets can be efficiently reduced by the PCA-based reconstruction. This PCA approach is very useful for analysis of atomic-column SI data, where unexpected signal correlations might be hidden over relatively high random noise due to the short acquisition time and the small analytical volume. This particular MSA plug-in package has been applied to various SI datasets acquired by EELS and EDS [1, 2, 11-13]. The package contains several useful utilities to deal with SI datasets more efficiently in DMS. Information about these and other details of the plug-ins are now available [14,15].

REFERENCES

1. *Bosman, M. et al. Phys. Rev. Lett. 99:086102, 2007.*
2. *Varela, M. et al. Phys. Rev. B 79: 085117, 2009.*
3. *Jeanguillaume, C. and Colliex, C. Ultramicroscopy 28:252-257, 1989.*
4. *Hunt, J. A. and Williams, D. B. Ultramicrosc. 38:47-73, 1991.*
5. *Kotula, P. G. et al. Microscopy & Microanalysis 9:1-17, 2003.*
6. *Jolliffe, I. T. Principal component analysis. 2nd Edn. Springer, New York, 2002.*
7. *Malinowski, E. R. Factor analysis in chemistry. 3rd Edn. Wiley, New York, 2002.*
8. *Cochran, R. N. and Home, H. Anal. Chem. 49:846-853, 1977.*
9. *Keenan, M. R. and Kotula, P. G. Surface and Interface Analysis 36:203-212, 2004.*
10. *Kimoto, K. et al. Micron 39:257-262, 2008.*
11. *Bosman, M. et al. Ultramicroscopy 106: 1024-1032, 2006.*
12. *Burke, M.G. et al. J. Materials Science 41: 4512-4522, 2006.*
13. *Watanabe, M. et al. Microsc. Microanal. 12: 515-526, 2006.*
14. *www.hremresearch.com/Eng/plugin/MSAEng.html*
15. *www.lehigh.edu/~maw3/research/msamain.html*